JET–R(98)10

H D Falter et al

60 kV Hydrogen Neutralisation Scan

JET–R(98)10

60 kV Hydrogen Neutralisation Scan

H D Falter, D Ciric, S Cox, D Godden.

JET Joint Undertaking, Abingdon, Oxfordshire, OX14 3EA,

December 1998

SUMMARY

To obtain the maximum neutralised fraction in the extracted beam requires a higher line density in the neutraliser than calculated from the cross sections. No evidence is found to support the hypothesis that the heating of the neutraliser gas by the beam is the main source for the observed reduced neutralisation efficiency. The theoretical maximum in the neutral fraction can be achieved at higher gas flows which are however associated with higher losses through charge changing collisions. Implantation and re-emission of gas in the neutraliser walls appears to have a strong influence onto the particle density of the neutraliser. There is clear evidence of space charge blow up in the ion beam at low densities, which complicates the interpretation of the measurements. The present deflection system on TB is found suitable for neutralisation measurements, however energy reflection has to be taken into account and the system is not sensitive to losses in the magnet.

1. INTRODUCTION

The observation that heavy molecules injected into the neutraliser do not contaminate the beam have led to a series of experiments aimed at increasing the neutralisation yield. The lack of neutralisation had been explained by the heating effect of the energetic beam on the neutraliser gas. Using heavy gases in the neutraliser could be beneficial for either increasing the line density in the neutraliser by slowing down the lighter hydrogen molecules or by more favourable cross sections. One significant advantage of a heavy gas could be that it can be pumped on LN_2 panels. The base pressure along the beam trajectory could be thus reduced which would also reduce losses through charge changing collisions.

The neutralisation scan in hydrogen reported here was intended as a benchmark for the more exotic tests. The evaluation focuses on examining our understanding and the suitability of the present set-up for neutralisation measurements.

2. EQUIPMENT USED

The experimental set-up is detailed in Table 1 and Fig. 1

Table1 : Set-up for the hydrogen neutralisation measurements.

PINI	11AT
date & pulses	10/06/98 = #103440-103480
deflection magnet	magnet with external coil installed in TT behind box scraper. Deflection downwards
method	PINI upshifted by 100 mm so that the undeflected beam lands mainly on the top half of the dump. The ions are deflected downwards by approximately 400 mm, landing partially on an inertial CFC dump extension

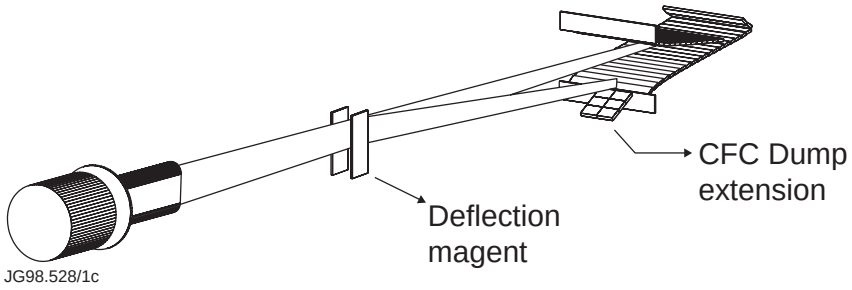

Fig,.1(a): Schematic of the TB deflection system

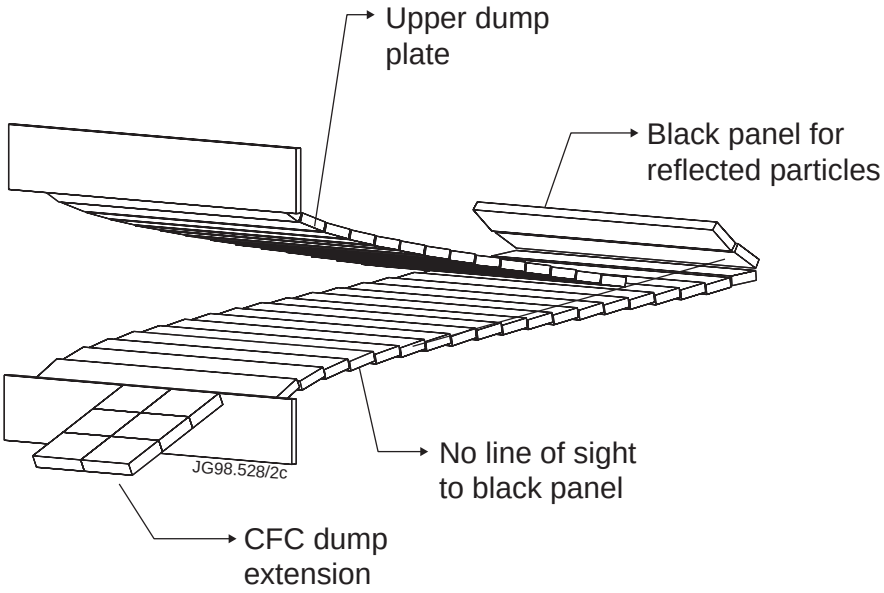

Fig.1(b): Blowup of the dump. From the front part of the bottom dump plate there is no line of sight to the back panel

3. CALCULATION OF LINE DENSITY

The line density is derived from flow scans [1] which give numerical expressions for the pressure at the start of the first stage neutraliser P_{N1}, the mid point of the neutraliser P_{Nm} and in the NIB P_{NIB}. The numerical expression has the form $P_v = a \bullet \Phi^b_{source} + c \bullet \Phi^d_{neutr} + e \bullet \Phi^f_{source} \bullet \Phi^g_{neutr}$.

The cross product is an artefact of the transition region in the neutraliser, which is not required for the NIB pressure (f = g = 0).

The parameters a - g are listed in table 2, Φ is the flow into the source or neutraliser in mbarl/s and P_v is the pressure in µbar. In the case of a beam the equivalent particle current of the extracted current has to be subtracted from the source flow. In this paper we use $1A \Leftrightarrow 0.145 mbarl/s$.

From the pressures the line density is calculated as

$$\Pi = 2.876 * 10^{13} * (L_{N1} * p^{av.}_{N1} + L_{N2} * p^{av.}_{N2} + L_{NIB} * p_{NIB}).$$

With L_{N1}=0.86 m, L_{N2}=1.00 m, and L_{NIB}=3.645 m we get:

$$\Pi = 2.876 \cdot 10^{15} \cdot \{0.86 * (p_{N1} + p_{nm})/2 + 1.00 * (p_{nm} + p_{NIB})/2 + 3.654 * p_{NIB}\} \; molecules / \mu bar * cm^2$$

This equation assumes that the pressure gradient is constant, which is not strictly true as the neutraliser is in the transition range. This procedure only yields 82% of the line density quoted in previous papers [2] (Fig. 2), which assumed the same conductance for both neutraliser sections.

Table 2: fitting constants to correlate the pressures in the PINI to the gas flows

	a	b	c	d	e	f	g
p_{N1}	0.382	0.96	0.145	0.94	-0.0097	0.6	0.94
p_{nm}	0.187	0.85	0.145	0.94	-0.0067	0.6	0.94
p_{NIB}	0.01068	1	0.01068	1	0.01432	0	0

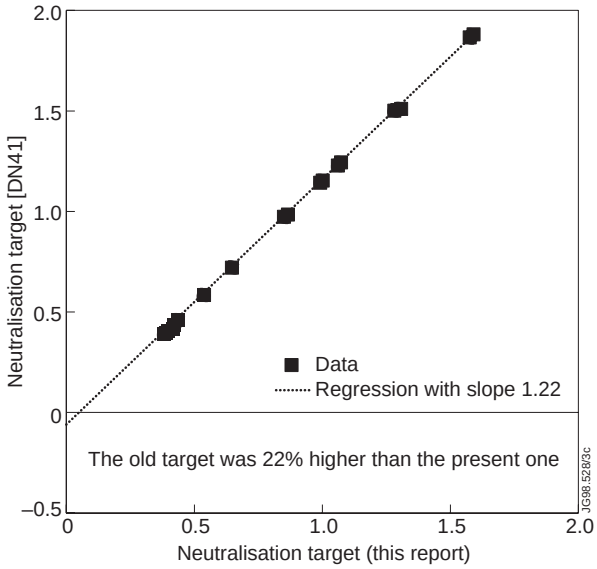

Fig.2: Comparison of the presently used estimate for the neutralisation target with that used in previous neutralisation scans [JET–DN–C(86)41].

4. EXPERIMENTAL PROCEDURE

The experiment was carried out with a 61 kV hydrogen beam operating at a perveance of $3.25 \pm 0.08 \mu perv$. The source gas flow was kept constant at 12.7 mbarl/s, the neutraliser flow was varied between 0 and 30 mbarl/s. The beam was upshifted by 100 mm. For each neutraliser flow a measurement was done with and without deflection. As Fig. 3 shows the ions are deflected by approximately 400 mm and the beams are essentially separated. However it should be pointed out, that the PINI used has a large vertical focal length showing the beams from the two grid halves still separated at a distance of 10 m and the separation of ions and neutrals is consequently not as good as it could be. The use of an inertial dump extension limits the pulse length to 3 seconds in this experiment.

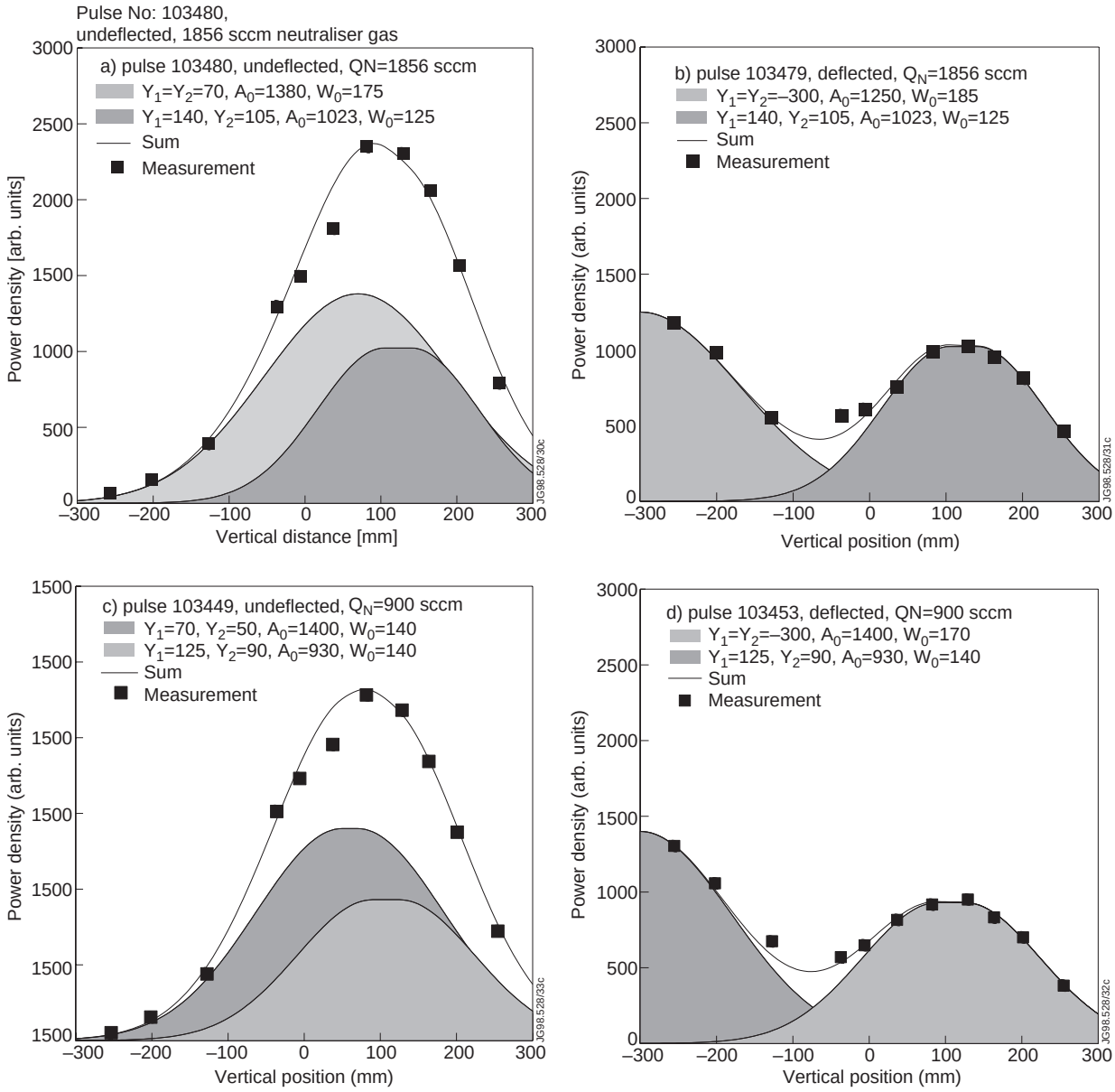

Fig.3: Beam profiles of deflected and undeflected pulses with medium and high gas flows.

4.1 Neutralisation measurement

The most straightforward way to measure neutralisation is from the power ratio on the top dump plate for deflected and undeflected beam which is essentially the definition used in previous experiments. In this experiment with upshifted alignment approximately 2/3 of the undeflected beam power end up on the upper dump plate. The neutralisation measurement based on the power on this plate is therefore only correct if deflected and undeflected beam have the same divergence and are not shifted against each other.

Alternatively the total neutral power can be estimated from the measured power on the top dump plate and from the beam profile and compared with the total power of the undeflected beam measured on both dump plates.

As Fig. 4 shows both definitions produce a lot of scatter at lower line densities. A reasonably good agreement between measurement and calculation is obtained if the power of the deflected beam on the upper dump plate is divided by the ***average*** power of the undeflected beam at higher flows. The reason for this scatter becomes obvious from Fig. 5 which shows that the transmission of the undeflected beam initially increases with line density while the losses decrease. Obviously space charge blow up of the ions limits the transmission at low pressures. At high line densities the transmission decreases and the losses increase with line density (pressure). This is likely to be a consequence of collisional losses in the accelerator [3]. An additional loss with increasing pressure occurs from charge changing collisions in the magnet. On TB this loss is likely to be small, as the ions are only deflected by a few degrees.

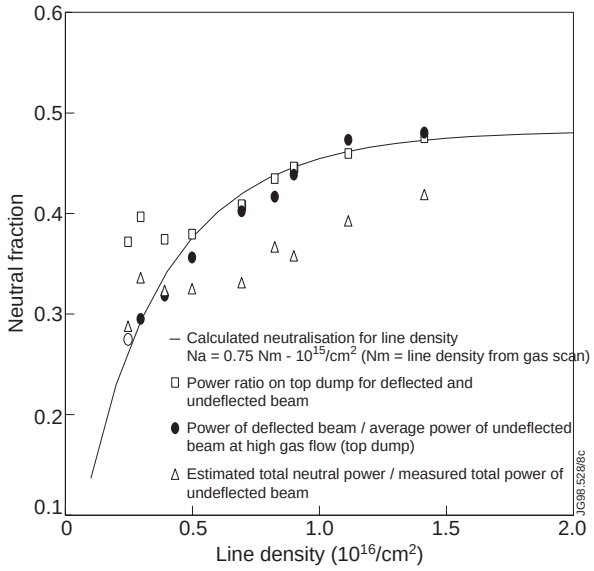

Fig.4: Hydrogen neutralisation scan PINI 11AT, #103443–480.

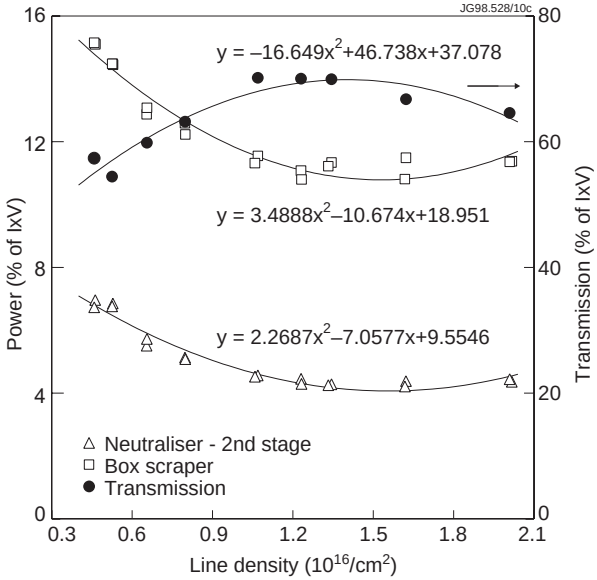

Fig.5: Power deposition as a function of line density PINI 11AT, Hydrogen.

4.2 Consequences of the space charge blow up.

The magnet on/off definition does **not** necessarily define neutralisation efficiency as both, transmission and ion/neutral ratio vary with line density. This is a common feature of all powerful neutral beam systems. Rather than following the physics approach we will restrict the evaluation to defining the parameters which yield the highest transmitted neutral power

5. OPTIMUM LINE DENSITY

From the neutralisation scan, one can either take the power on the top dump, or the estimated total neutral power (estimated from the measured power on the top dump and from the profile). The top dump extends over a width of 30<y<300 mm. Taking the neutral profiles in Fig.3 the estimated neutral power is $p_{estimated} = p_{measured} * \int_{-300}^{300} fitfunction / \int_{30}^{300} fitfunction$, where

fitfunction is the fit on the deflected beam shown in Fig. 3 . The result is shown in Fig. 6. Using a quadratic fit through the data points and assuming that the measured neutral power is only 95% of the actual neutral power because of energy reflection (Annex 1) we get the transmitted power in Fig. 7. As in [4] we assume 4% magnet loss per 10^{20} m^{-2} line density. The power from the top dump has much less scatter and is therefore suited best to define the optimum line density which is 2 10^{20} molecules/m^2. The total neutral power is very close and within the error margin of what we can expect from the cross sections and the losses.

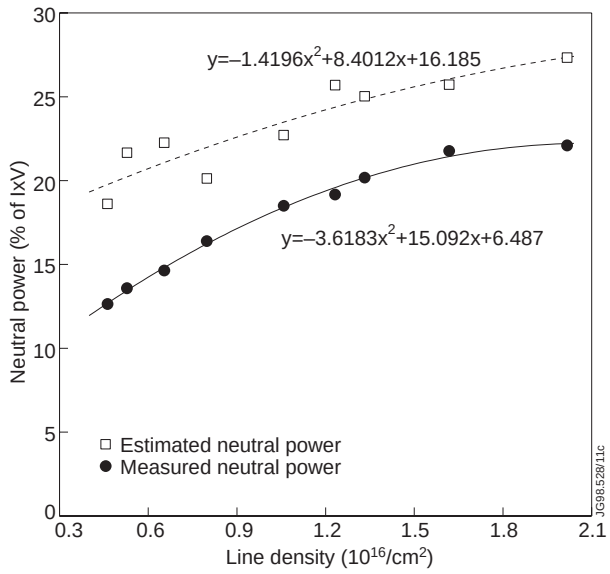

Fig.6: Estimated neutral power as percentage of the extracted power (60 kV Hydrogen).

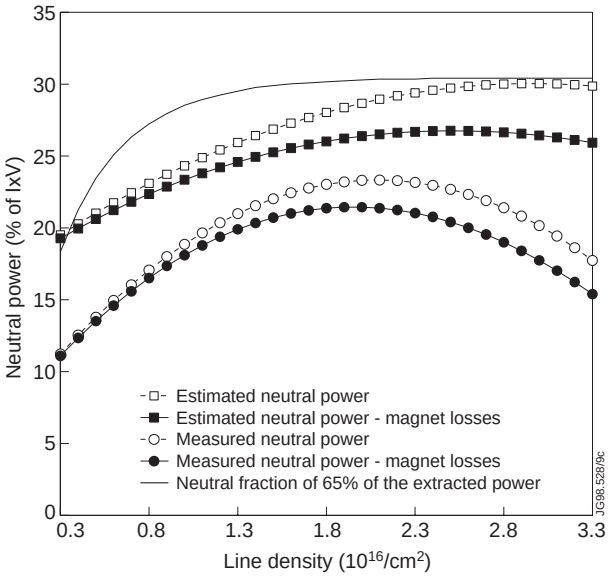

Fig.7: Comparison of the measured and expected neutral power. PINI 11AT, Hydrogen, 61 kV, #103449 – 103480 magnet loss: 4% at 10^{16} line density.

6. EVIDENCE FOR AND AGAINST BEAM HEATING OF GAS IN THE NEUTRALISER

The requirement of higher gas flows has led to the postulation that the neutraliser gas is heated by the beam and that the actual gas density is correspondingly reduced [4,5]. An upper limit of the beam heating can be derived from the hydrogen stopping power in hydrogen gas which yields a loss of 128 eV for a 61 kV hydrogen beam and a line density of 10^{20} Molecules/m^2 [6]. At a current of 50A the maximum energy loss is therefore just above 6 kW. This compares with a heating power of 100 kW in the source just from the arc power.

6.1 Neutraliser pressure

6.1.1 What should we see

A change in gas temperature changes almost everything: density, viscosity, mean free path. The neutraliser operates in the molecular range and in the transition range. The Knudsen formula calculates the pressure drop in all ranges (molecular, viscous and transition), but the complete component has to be in the same range. If we split the neutraliser in small sections with the

length L_v we can satisfy the condition that the complete section is in the same range and the pressure can be calculated in steps.

The flow Φ is kept constant and the conductance C_v is defined by $C_v = \Phi/\Delta p = \Phi/(p_v - p_{v-1})$. The Knudsen formula is given by Roth [7] in the form

$$C = \frac{\pi \cdot D^4 \cdot \frac{P_v + P_{v-1}}{2}}{128 \cdot \eta \cdot L_v} + \frac{1}{6}\sqrt{\frac{2\pi RT}{M}}\frac{D^3}{L_v} * \frac{1 + \sqrt{\frac{M}{RT}} * \frac{D \cdot (P_v + P_{v-1})}{2 \cdot \eta}}{1 + 1.24 * \sqrt{\frac{M}{RT}} * \frac{D \cdot (P_v + P_{v-1})}{2 \cdot \eta}} \qquad (5).$$

The viscosity η is temperature dependent:

$$\eta = \frac{0.998}{\pi \varsigma^2}\sqrt{mkT/\pi}/(1 + \frac{c}{T})$$

By introducing the quantities α, β, γ, which are products of the constants in (5) and the temperature, the Knudsen formula simplifies to

$$C_v = \alpha(P_v + P_{v-1}) + \beta * \frac{1 + \gamma(P_v + P_{v-1})}{1 + 1.24\gamma(P_v + P_{v-1})}$$

which leads us via $P_n = P_{n-1} + \frac{\Phi}{C_n}$ to the expression

$$P_n = P_{n-1} + \Phi \Big/ \alpha(3P_{n-1} - P_{n-2}) + \beta \frac{1 + \gamma(3P_{n-1} - P_{n-2})}{1 + 1.24 \cdot \gamma(3P_{n-1} - P_{n-2})}$$

By assuming a constant gradient we use $(P_n + P_{n-1}) = (3P_{n-1} - P_{n-2})$ in the expression above which can be iterated with a suitable boundary condition for P_{-1} and P_0.

List of symbols used in the Knudsen formula with numerical values for one particular temperature

M	mass/Mol [gr/Mol]	2.016
R	gas constant [erg K^{-1} mol^{-1}]	8.315E+07
T	temperature [K]	100...1800
L	length increment [m]	0.01
D	equivalent diameter [m]	0.3586
ς	molecular diameter [m]	2.68E-10
c	Sutherland constant.	76
m	hydrogen mass [kg]	3.345E-27
k	Boltzmann constant [erg K^{-1}]	1.3804E-16
Φ	flow [μbar m^{-3} s^{-1}]	250
η	viscosity [poise]	5.3621 10^{-5}

Fig. 8 shows the pressure distribution calculated from the Knudsen formula for temperatures between 100 and 1800 K using the equivalent diameter of the neutraliser. The pressures are in the right range and the curves show, that we move towards the molecular range with increasing temperature (the pressure gradient becomes more constant). The main result of this calculation is, that the pressure **decreases** with increasing temperature.

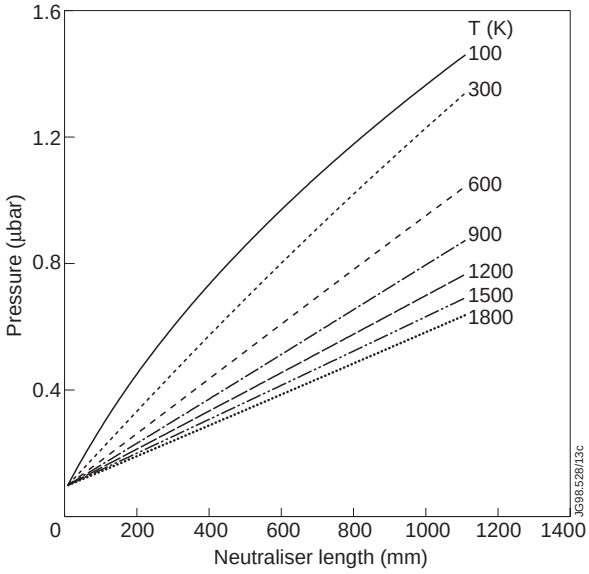

Fig.8: Pressure drop through the first stage neutraliser for 25 mbarl/s pressure calculated from Knudsen formula in steps of 1cm. Parameter is the temperature.

The calculation above is for a pipe in steady state conditions with a fixed flow rate. As will be shown later, the temperature rise with beam on is expected to be much faster (1000 ^{o}K/ms) than the time constant for the pump out. We would therefore expect an initial pressure spike when the beam comes on, which decays to the steady state value with the pump out time constant of the system (200 - 400 ms).

6.1.2 what do we see

On the test bed we routinely measure the pressure in the gap between first and second stage neutraliser with a Baratron. This Baratron is installed at a port of the gate valve isolating the PINI from the tank. The baratron is at room temperature and the measurement might be influenced by thermal transpiration: When a hot chamber is connected to a cold chamber with an opening smaller than the mean free path, the particle flux in either direction must be same. This requires $p_{cold} = p_{hot} * \sqrt{T_{cold}/T_{hot}}$ to be valid. If gas - gas collisions dominate the pressure measurement is not affected by temperature gradients.

The pressure development in the neutraliser for a wide range of gas flows is shown in Fig. 9 together with a typical beam current. All pulses had the same source gas flow and beam current, whilst the neutraliser gas flow was varied. At low gas flows there is a pressure drop when the beam comes on, at higher flows the pressure rise with beam on. Characteristic pressures at the times marked in Fig. 9 are shown

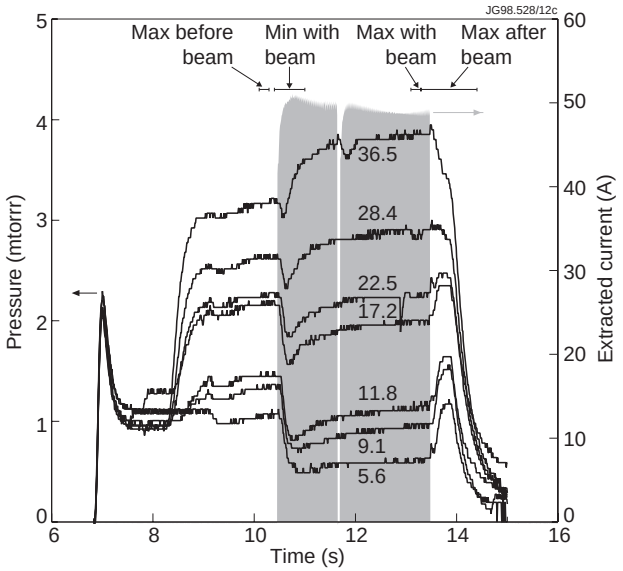

Fig.9: Pressure between first and second stage neutraliser source flow: 12.7 mbal/s, neut. Flow: 0–31 mbl/s, beam current: 50A, Hydrogen.

in Fig. 10 for the pressure before beam on, the minimum pressure with beam, the maximum pressure with beam, and the highest pressure after the beam has gone off. These pressures are compared with those from the gas scan. The pressures measured in the neutralisation scan are all lower than those from the gas scan, which can be explained by the longer pulses used in the gas scan and by the pumping of the arc in the plasma source. To make both measurement comparable we adjust the equilibrium pressure from the gas scan to fit the measured pressure before beam in the neutralisation scan, which requires a reduction in slope by a factor 1.11 and a shift of 0.0001. If we use the same correction for the pressure expected with beam we get a reasonable agreement with the measured minimum pressure at the start of beam extraction (graph on the left). This means that we do not see an effect of increasing gas temperature when the beam comes on, either because it is too small or it is compensated by thermal transpiration. The picture changes completely if we look at the end of the beam pulse (graph on the right). Both, the pressure at the end of the beam pulse and the pressure after the beam has gone off show a stronger increase with flow than expected from the gas scan and rise to values well above those expected from the gas scan.

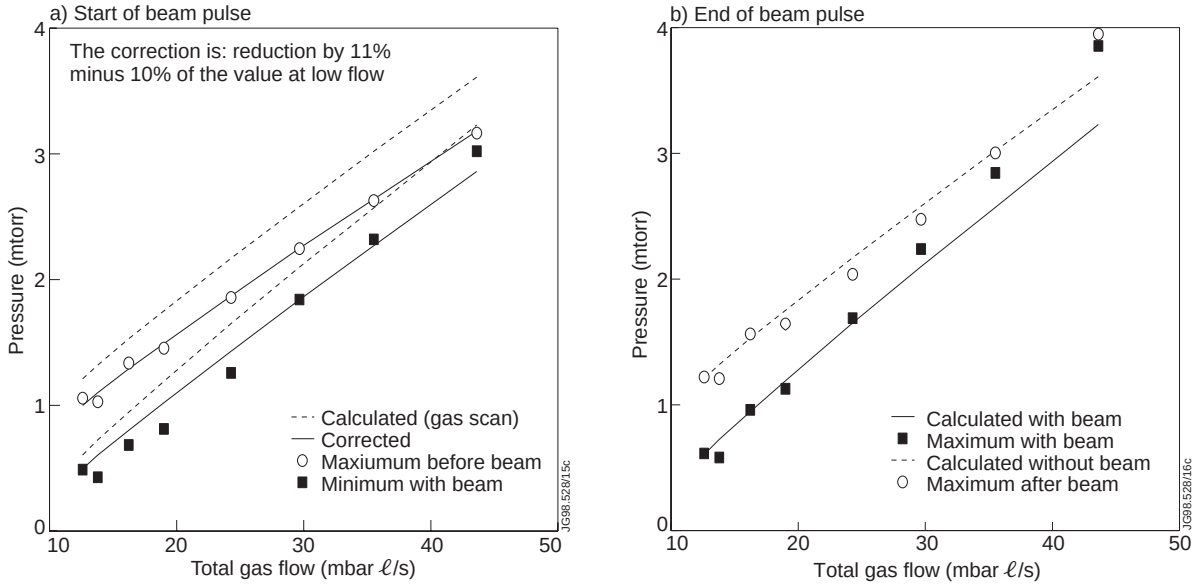

Fig.10: Characteristic pressures in the neutraliser with beam compared with the pressure from the gas only scans.

Fig. 11 shows the pressure of the pulse with the highest gas flow together with the exponential time constants for the various changes in pressure. All the time constants are very similar. In particular the pressure rise with beam has a time constant of 0.35 seconds and the pressure decay when the beam goes off has a time constant of 0.2 seconds[1]. These long time constants are difficult to understand, if gas heating were to be the source of the change in pressure. At a line

[1] In an experiment with hydrogen in the source and Neon in the neutraliser the time constants increased to approximately 1 s as expected from the square root of the mass ratio. This shows that 0.2 s is not the instrumental time constant.

density of 2 10^{20} atoms/m^2 we have a total of 2 10^{19} atoms in the neutraliser. The specific heat of this gas is 0.335 mWs/ ^{0}K. With a heating power of 3 kW one would expect a time constant of $335 \cdot 10^{-6} \frac{Ws}{K} / 3000W = 1.12 \cdot 10^{-7} \frac{s}{K}$. Even if only 1/3 of the dissipated energy is transferred into thermal energy we would expect a temperature rise of the order of 3000 ^{0}K/ms.

Both, the gauge (MKS Baratron type 51A) with a response time < 0.02 second and the time constant of the conductance through the gap between first and second stage neutraliser with $200l \div 30000\, l/s = 6.7 * 10^{-3} s$ are fast compared with the measured times above.

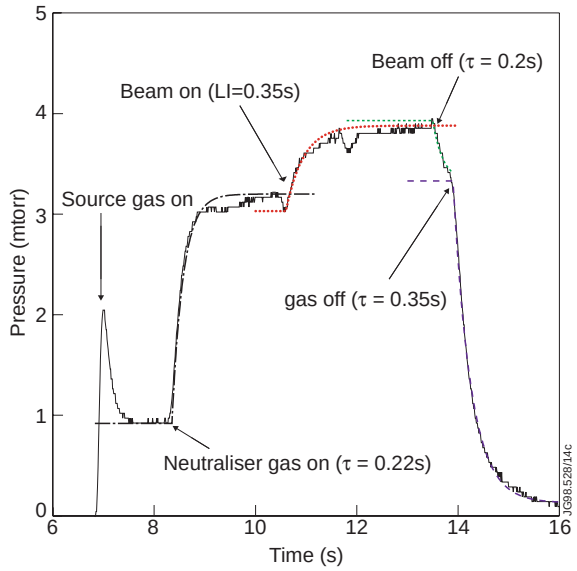

Fig.11: Time constants for pressure changes in the neutraliser #103480, pure hydrogen pulse (pulse with highest neutraliser flow).

6.1.3 simplified numerical example

In this example we drop the assumption that the heating of the neutraliser gas will result in a hotter bulk gas with a fully developed Maxwell distribution. The mean free path in the neutraliser is of the order of 50 mm and most particles are within one mean free path of the wall. We assume, that there will be a hot population and a cold population in the neutraliser gas. A full treatment would require a Monte Carlo simulation, which is beyond the scope of this paper. Instead we will use some simplifying assumptions.

At a line density of 2 10^{20} atoms/m^2 in the neutraliser the hydrogen stopping power for a 60 kV ion is 128 eV. In these collisions the fast ion produces on average two ions in the target gas. This means that 100 eV is left for radiation and for heating. Neglecting radiation, we use 100 eV for heating. A 50A beam produces 5 kW of heating. With 2.6 m^2 of wall surface the heat flux to the wall is 1.92 kW/m^2.

The gas kinetic cross section of hydrogen is 6 $10^{-20}$$m^2$, so each fast particle has 6 collisions and transfers 16.67 eV/collision on average. Further we assume a cascade of 4 collisions in which the energy is equally spread over the 2^4 collision partners which end up with 1 eV each.

We now have the energy balance $\frac{n}{4} c_{av} * \Delta E = 1.92\, kW/m^2$. With $c_{av} = 10^4$m/s corresponding to ΔE = 1 eV we get n_{fast}=4.8 10^{18}/m^3, where n is in molecules/m^3. This compares with a cold density of 10^{20}/m^2/1.86m = 5.376 10^{19}mol/m^3. The fast population is **9%** of the initial density.

This fast population would influence the pressure measurement as follows: The Baratron is in a volume of 0.2 m^3 outside the neutraliser connected by a gap of 0.2x1.4 = 0.28 m^2. The flux balance across this gap is: $\frac{n_{fast}}{4} c_{fast} + \frac{n_{slow}}{4} c_{slow} = \frac{n_{bar}}{4} c_{slow}$ (n_{bar} is the density at the Baratron. The thermal velocity is 1.93 10^3 m/s and we get n_{bar}/n_o= 1.37. This means that we expect a 37% pressure rise from thermal transpiration.

Finally the time constant of this pressure rise is defined by the flux and the volume: With the numbers above we get $dn/dt = 1.68 \cdot 10^{22}\, m^{-3} s^{-1}$. With a start density of 5.376 10^{19}m^{-3} this gives a time constant of 3.2 ms.

To conclude: The heating of the neutraliser gas should manifest itself in a fast pressure rise. If the fast particles do not equilibrate fully with the cold background gas then the effect on the density is likely to be insignificant.

To complicate matters further, Fig. 12 shows the pressure in the NIB and in the neutraliser for two pulses with identical gas flows. In pulse 104032 the power supplies tripped at the start of beam extraction, pulse 104049 was a pulse with 52 A of extracted current. The gas flow was 26 mbarl/s the equivalent gas in the beam is 7.5 mbarl/s and one would expect a pressure drop of 29% in the NIB if all the beam current were implanted without any associated degassing. The measured pressure drop is twice as high indicating that half the gas is initially not streaming into the NIB. During beam on the pressure rises in the NIB with a slow time constant. If the change in neutraliser line density would only be caused by gas heating, we should see no change in the NIB pressure. This shows clearly that other effects are dominating the variation in line density.

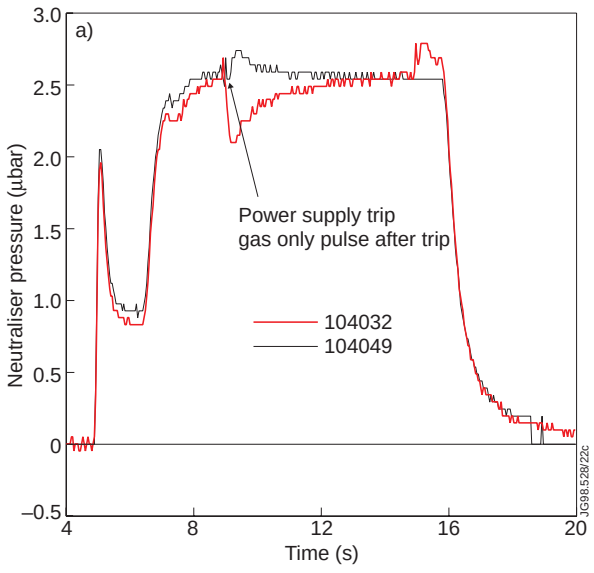

Fig.12 (a): Neutraliser pressure with and without beam.

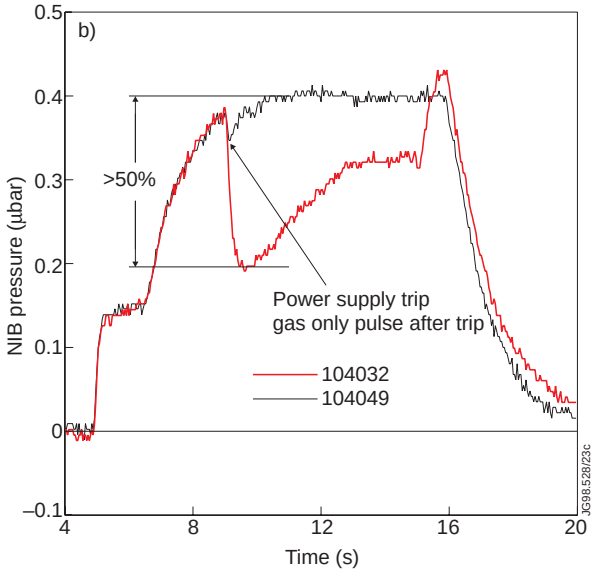

Fig.12(b): NIB pressure with and without beam.

6.2 G3 current as density sensor

The current on the repeller grid is mainly drawn from the neutraliser plasma. This can be deduced from a power balance on the repeller grid. The normalised G3 current (normalised to the extracted current and with the ohmic current subtracted): $I_{G3n} = (I_{G3} - 1050\Omega / U_{G3}) / I_{extr.})$ shows a positive spike at the turn on followed by a slow rise to the equilibrium value (Fig.13).

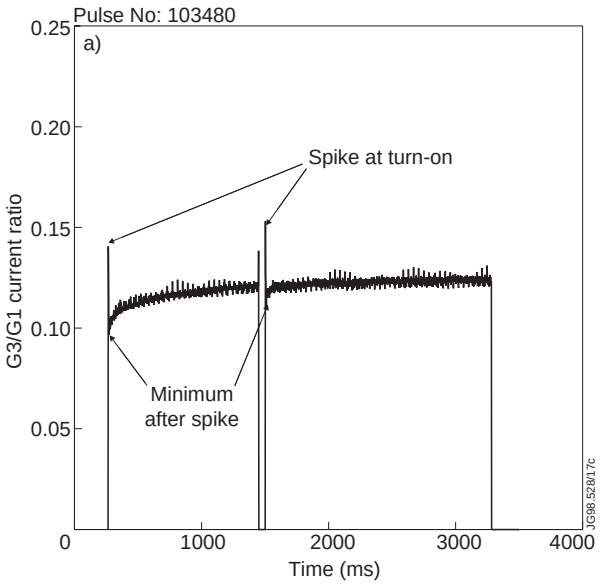

Fig.13(a): Normalised G3 current waveform, showing an initial spike, followed by a slow current rise.

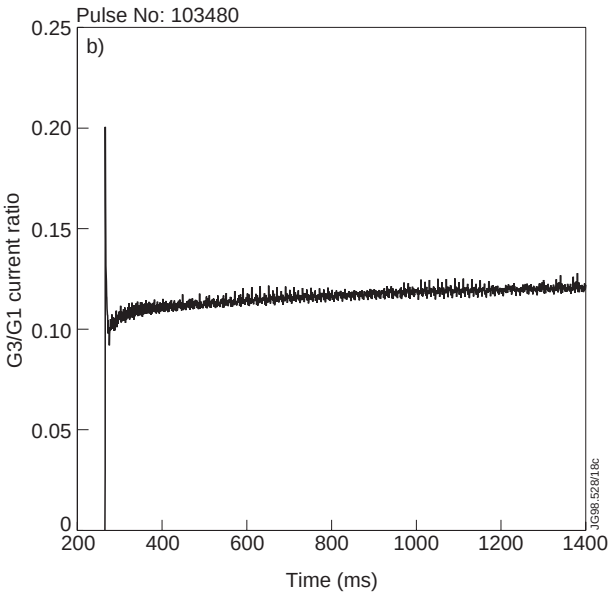

Fig.13(b): Normalised G3 current waveform. The decay of the initial spike is fast, the following rise has two time constants. The initial faster rise has a time constant of 40ms and an amplitude of 0.01, the slower rise has a time constant of 1000ms and an amplitude of 0.016.

The slow current rise during beam on follows exactly the pressure rise in the neutraliser (Fig. 14). From this we can conclude, that the pressure rise during beam on is a density rise - not a temperature rise.

The initial spike in G3 current decays first with a time constant of 0.8 ms which is independent of the gas and then with a time constant of 3ms with hydrogen in the neutraliser and 5.5 ms with Neon in the neutraliser (Fig. 15). The small time constant of the spike is indicative of a fast density reduction. However gas heating can not cause this fast reduction in density as the gas has to flow out of the

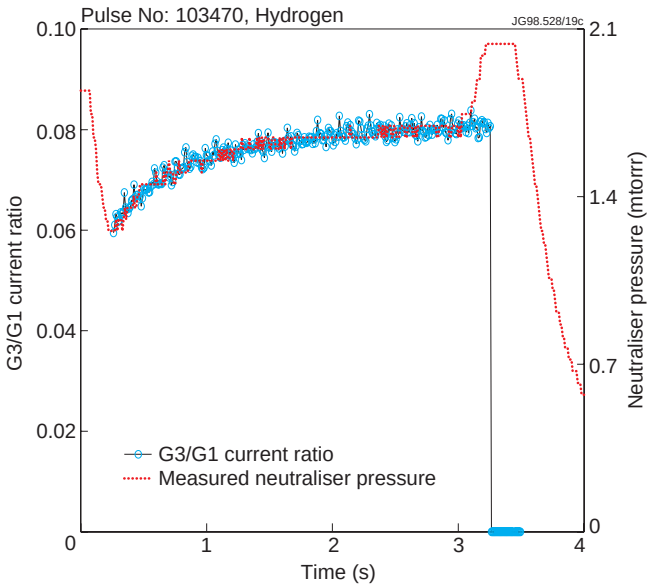

Fig.14: Comparison of the pressure rise in the neutraliser with the current rise on the repeller grid.

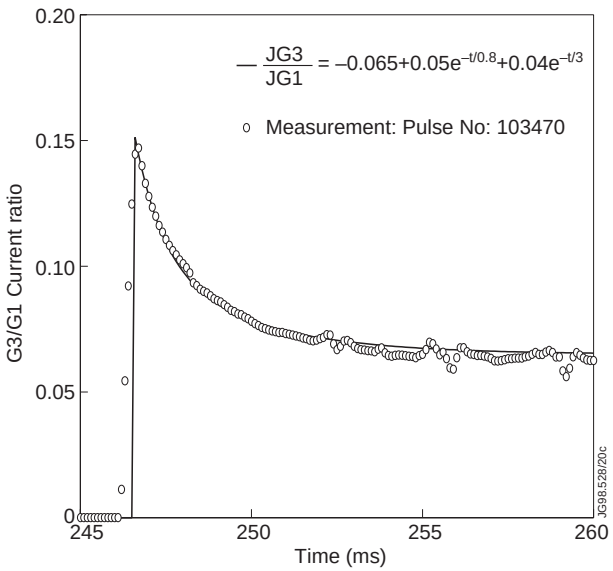

Fig.15(a): Time constant of the spike on G3 current – hydrogen pulse.

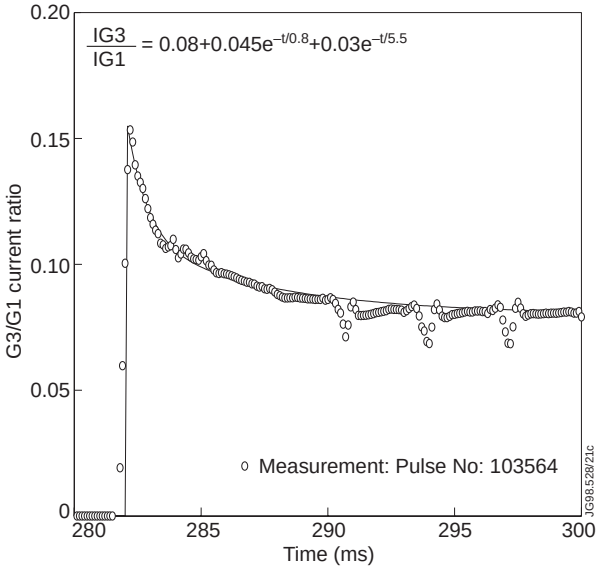

Fig.15(b): Time constant of the G3 current spike – hydrogen/neon pulse.

neutraliser. All characteristic G3 current values (spike, minimum with beam and maximum with beam) and the power loading on G3 increase linearly with neutraliser pressure (Fig. 16) following a linear offset law. As the currents are proportional to density this means that the pressure variation with beam is a density variation (the pressure in Fig. 16 is taken from the gas scans).

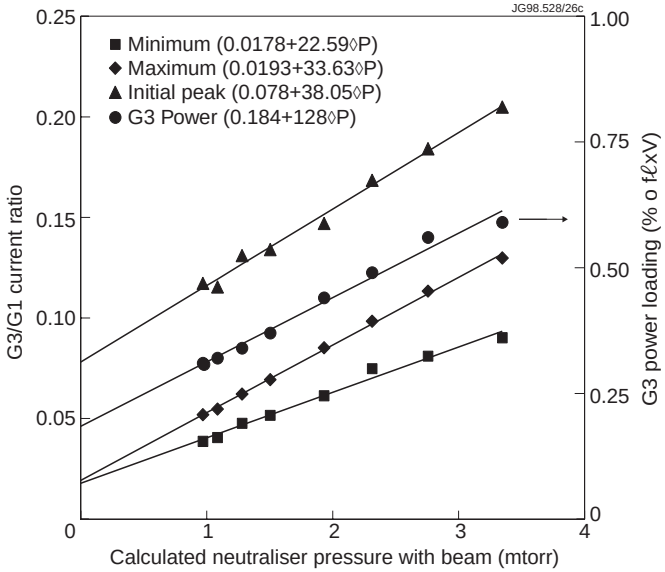

Fig.16: Variation of the G3 current with pressure # 103360 – 380, Hy6drogen, 50 A.

7. CAN IMPLANTATION AND RE-EMISSION EXPLAIN THE OBSERVED PRESSURE TRACES?

Implantation and re-emission can be substantial and there is some evidence available from previous papers:

1. Operating TB as a closed volume using recirculating gas shows that the loss of gas per beam pulse is initially 10 times the gas transported in the beam, decaying over some ten pulses to approximately twice the gas transported in the beam [8]. This is a global observation from pressure measurements in the in the vacuum tanks (pressure before and after a pulse).

2. From the build up of deuterium in the dumps, measured via the neutron emission from beam target collisions, we know, that implantation is limited by a density limit which is reciprocal to the surface temperature. The observed limit is typically 10 - 20% of the density of the target material and the build up and clean up is well explained by the local mixing model [9] which assumes that everything is implanted up to the saturation density. Once the saturation density is reached the emitted flux equals the implanted flux.

As the saturation density is reciprocal to the wall temperature, this means that at the beginning of a pulse all the flux is implanted. The wall heats up and after a certain time the density will have reached the temperature dependent saturation density at which implantation equals re-emission. The wall might heat up further, the saturation density drops and the there is a net remission. At the end of the pulse the wall will cool down to room temperature, and between pulses some of the implanted gas will be released. This means, that the wall is always unsaturated at the beginning of the pulse, but it will depend on the previous exposure when the saturation density is exceeded and a net re-emission sets on.

In the neutraliser the power deposition is not equally distributed. Areas with a high power loading will already be saturated while less exposed areas might still pump. The transition from a pumping wall to an emitting wall is therefore gradual. There are also semi inertial sections which could reach the peak temperature after the pulse and would therefore still be emitting when the beam goes off. Additionally diffusion increases strongly with temperature and contributes to the re-emission.

With the above in mind, the pressure traces in Fig. 11 show qualitatively what one would expect with pumping neutraliser walls:

- the time constant for the pressure drop with beam is shorter than the time constant for a pump out through the neutraliser exit as the path length to the wall is shorter.
- The implantation flux to the neutraliser increases with line density. The higher the density, the earlier the saturation limit will be reached and the pressure will start to rise.

The upper limit of possible implantation can be estimated from the ionisation cross section of the H_2 gas in collisions with fast beam ions and neutrals: At a line density of 10^{20} molecules/m^2 each fast beam particle produces two slow H_2^+ ions[2]. A beam of 50 A produces 100A of slow ions which corresponds to a gas flow 23 mbarl/s, which is above the flow required for a line density of 10^{20} molecules/m^2.

The experience of hydrogen implantation in copper is from energetic beam particles (50 - 150 keV). In the neutraliser the ions are at a much lower energy (probably 1 - 10 eV). We know

[2] For this estimate it is assumed that the beam consists of full energy particles only and that 80% of the beam particles are ions.

from the pressure loss before and after beam extraction in a closed system, that not only energetic beam particles are being implanted, but we have not yet made an attempt to develop a quantitative model.

8. DISCUSSION

It is not disputed that the neutraliser gas absorbs energy from the beam. The question is which energy distribution will evolve in the neutraliser gas. The problem might become obvious from the following estimates:

Taking an average pressure of 2 μbar and the gas kinetic cross section of hydrogen of 5.6 10^{-20} m^2, we get 1.8 10^{21} collisions/second between a 50A beam and the neutraliser gas. This compares to 6.7 10^{22} collisions between the neutraliser gas molecules and the wall. In a collision between a fast beam particle and the background gas the energy transfer is likely to be in the eV range. To create a hot gas from these collisions would require that the energy is dissipated among all the molecules in the neutraliser. The mean free path in the neutraliser (Fig. 17) is between 30 and 100 mm. Taking 50 mm as average, 60% of the molecules are within one mean free path of the wall. Assuming that the gas could reach temperatures of 1200 K, the density would go down by a factor of 4 and the neutraliser would be completely in the molecular range.

Instead of a Maxwell distribution we will rather have a minority of energetic particles, which make the energy transport to the wall, and a majority of thermal particles, which dominate the density in the neutraliser. However, approximately 100 A of ions are created in the neutraliser which is comparable to the total gas flow and could result in significant implantation.

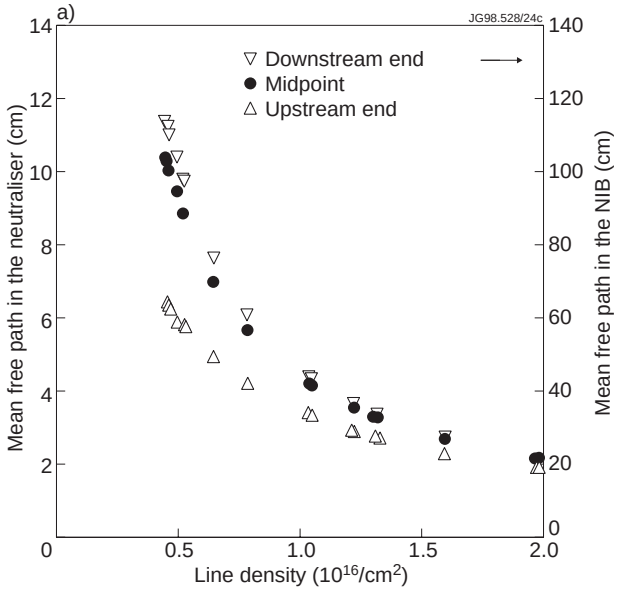

Fig.17(a): Mean free path in the neutraliser at 300 K. Calculated for the flows used in the Hydrogen neutralisation scan.

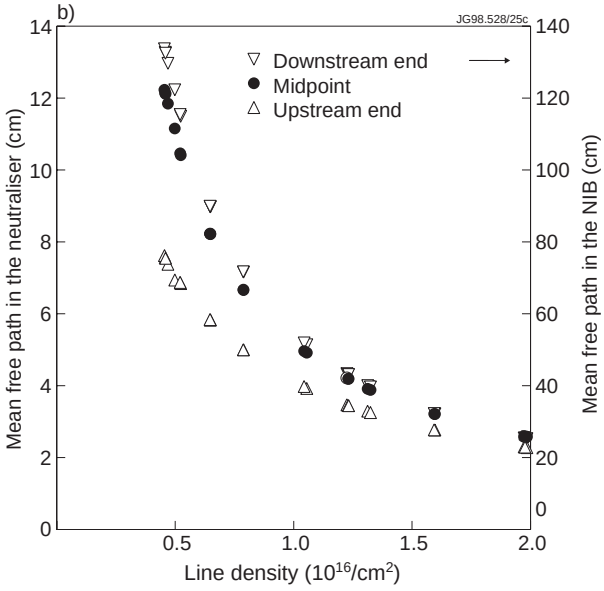

Fig.17(b): Mean free path in the neutraliser with 1200 K for Sutherland correction. The density is kept constant as for 300 K, only change is in Sutherland correction.

Gas heating and implantation/re-emission both influence the measured pressure in the neutraliser. The main effect of the gas heating is probably an increase in the measured pressure due to thermal transpiration, while the reduction in density is probably mainly caused by implantation and is larger than the measured pressure drop.

Apart from energy the beam also transfers momentum to the neutraliser gas. Additionally, as we neutralise part of the ion beam in the neutraliser we get a reduction of the electrical current along the length of the neutraliser. This means, that there is a gradient in fast ion density which has to be compensated by electrons. A confining electrical field for the electrons must therefore be present.

9. CONCLUSIONS

1. The neutraliser line density was overestimated in the past as there were no measurements of the conductance of the first stage neutraliser. It might still be overestimated in this paper as the actual gas stabilisation times are too short for equilibrium values.
2. The theoretical neutralised fraction can be achieved but the gas flows required are higher than expected from the conductance of the neutraliser. At these higher flows losses through charge changing collisions in the accelerator grids limit the actually obtainable neutral power.
3. The deflection magnet used in the test bed is not sensitive against losses and is therefore not suitable for measuring the benefit from neutraliser gases which can be pumped on liquid nitrogen panels.
4. A powerful neutral beam system is not suitable for measuring the relation between neutralisation efficiency and line density as space charge effects at low densities distort the measurement.
5. There are no direct observations which support the gas heating theory.
6. Gas heating on its own is unsuitable for explaining the mismatch between expected and required neutralisation line density.
7. Gas implantation in the neutraliser is probably the dominating effect but further work is required to quantify this.

10. ANNEX 1: ENERGY REFLECTION ON THE TB BEAM DUMP

Reflection of energy can distort the power measurement on individual plates of a V shaped dump if either the system is not symmetrical with respect to the horizontal plate or if the beam is not centred with respect to the dump axis. For the neutralisation measurements on TB neither condition is fulfilled and the measured power deposition has to be corrected.

The test bed beam dump(Fig. 1) consists of 3 panels. The top panel has 14 vapotron beam stopping elements, the bottom panel has 18 beam stopping elements plus one inertial section, and the back panel two vapotron elements. The reflection of energy was calculated by Eckstein [10] for Deuterium on copper. For 80 kV and 82^0 angle of incidence (normal incidence $\Leftrightarrow 0^o$)

the calculated energy reflection coefficient is 0.17, however the author emphasises that the “real surface may be quite different from those used in the computer simulation. This may lead to lower reflection coefficients, especially for large angles of incidence”.

By steering the beam vertically up and down and measuring the power on the three plates of the dump, one can get the following estimates for energy reflection:

10.1 Back Panel

The power ratio between bottom plate and back panel is shown in Fig. 18 as a function of vertical beam steering: The fraction of power on the back panel increases when the beam is shifted upwards until the beam centre reaches the upper plate. A further shift upwards leads to a small reduction in power on the back panel. To understand this observation one has to remember that

1. Only particles from the bottom plate can get to the back panel.
2. Both, angle of incidence on the bottom plate and the acceptance angle for the back plate decreases when moving from the centre to the edge (see Fig. 1).

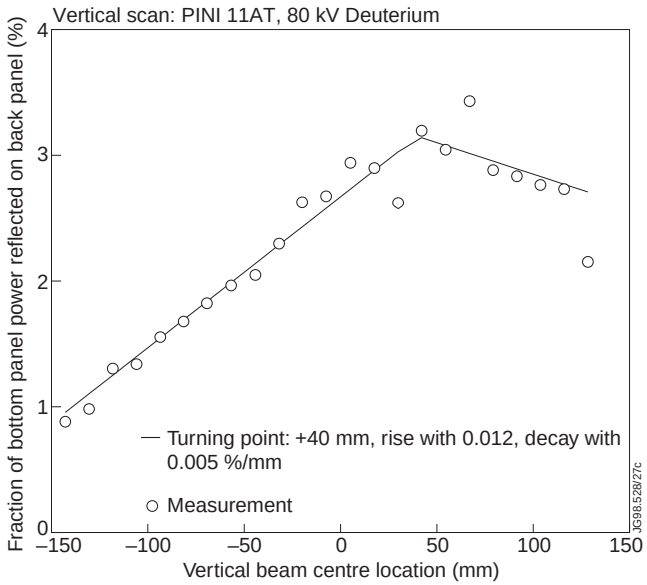

Fig.18: Power on the back panel in a vertical scan PINI IIAT, 80 kV Deuterium.

The increasing power fraction with vertical upshift is obvious with 1. and 2. as the beam centre moves from the outer parts to the centre of the dump. Once the power is mainly on the top dump, an increasing fraction of power on the bottom dump plate is from reflected particles from the top dump plate. These particles have a smaller angle of incidence and therefore a lower probability to reach the back plate. We can therefore conclude:

1. As 3.15% of the power on the bottom plate end up on the back panel, the reflection coefficient must be at least 0.0315.
2. As not all particles reflected from the bottom plate get to the back panel the reflection coefficient must be well above 0.0315.

10.2 Relation between measured and actual power on the upper and lower dump plates.

With the nomenclature in table 3 we can write:

$$P_{upper} = P^r_{upper} \cdot (1-\gamma) + P^r_{lower} \cdot \gamma\,, \tag{1}$$

$$P_{lower} = P^r_{lower} \cdot (1-\gamma) + P^r_{upper} \cdot \gamma \tag{2}$$

These equations yield

$$P^r_{upper} = \frac{\frac{1}{1-\gamma} P_{upper} - \frac{\gamma}{(1-\gamma)^2} P_{lower}}{\frac{1-2\gamma}{(1-\gamma)^2}} \tag{3}$$

$$P^r_{lower} = \frac{1}{1-\gamma} P_{lower} - \frac{\gamma}{1-\gamma} P^r_{upper} \tag{4}$$

The calculated "real" powers on the two dump plates are plotted in Fig. 19 together with the measured powers for a reflection coefficient of 0.07 and 0.1, which can be regarded as an upper limit as the power on the top plate goes to zero for the largest downward steering (no intersection with the top plate). 7% appears to be a good estimate, with the reflection coefficient being well above 3% (back plate measurement), and not above 10%.

Table 3: Nomenclature for energy reflection

P_{upper}, P_{lower}	measured power on the upper and lower dump plate
P^r_{upper}, P^r_{lower}	real power on the upper and lower dump plate
γ	energy reflection coefficient

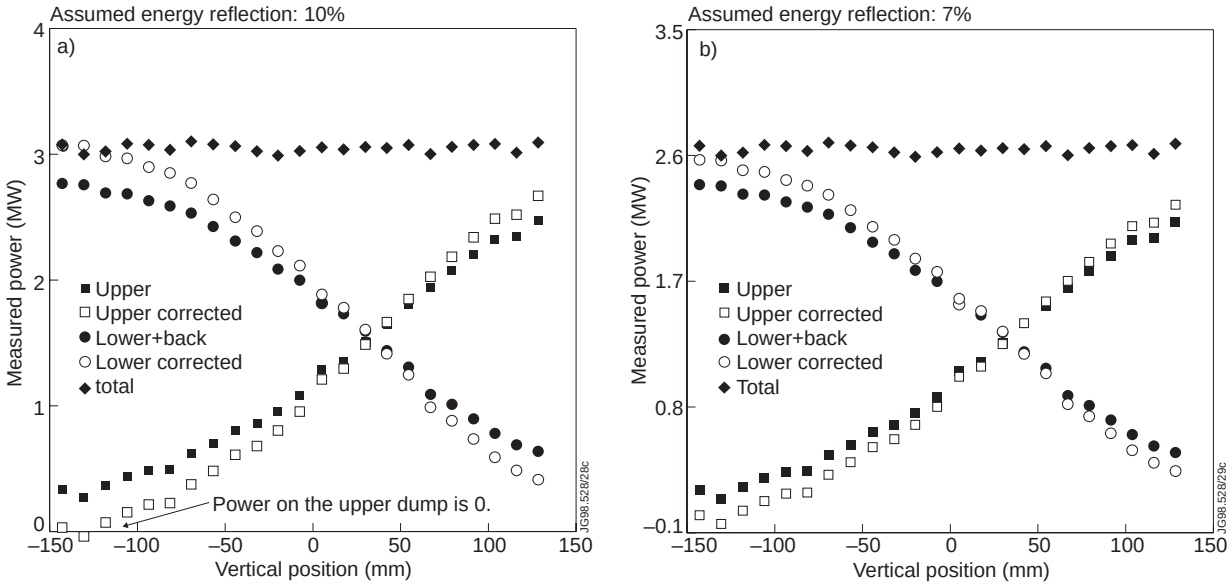

Fig.19: Measured and estimated power on the upper and lower dump plate.

REFERENCES:

[1] D Ciric - gas flow scans in the NB test bed - Measurement and interpolation formulae. In preparation

[2] Hemsworth, R "Calculation of the gas target in the neutraliser in the absence of any 'beam effects'", JET-DN-C(87)41

[3] D CIRIC “Losses in the accelerator of neutral beam injectors caused by charge changing collisions, JET-Report (in preparation), see also: D Ciric, “Space and time resolved Doppler spectroscopy of neutral beams”, Proceedings of the 20th SOFT conf. Sept. 7 - 11 (1998), Marseille

[4] A Staebler, “Comparison of experimental and predicted neutralisation efficiency for the JET beam system” - JET-DNC(85)14,
R S Hemsworth, “Neutralisation Measurements for the JET Injectors”, Proc 13th Conf on Contr Fus and Plasma Heating, Schliersee, FDR, 1986, pp297-300

[5] J R Pamela, “Gas Heating Effects in the Neutralisers of Neutral Beam Injection Lines”, Rev Sci Inst 57 (6) 1986, pp 1066 - 1068

[6] H H Andersen, J F Ziegler, “Stopping power and ranges of ions in matter, Vol. 3, New York, Pergamon Press, 1977

[7] A. Roth, Vacuum Technology, North-Holland Publishing Company, 1976

[8] H D Falter et al, “Implantation and re-emission of hydrogen and helium in the beam stopping panels of a 10 MW ion beam line”, Journal of Nuclear Materials 176&177 (1990) 678-682

[9] H D Falter et al, “Hydrogen isotope exchange in the JET Neutral Injection System”, presented at the 17th SOFT, Rome, Italy, 14-18 Sept. 1992, pp481-485.

[10] W Eckstein, Computer simulation of reflection of hydrogen and deuterium from Cu, JET-Contract JC1/9012 - Final Report (1981).